Development and Evaluation of BaFe$_{12}$O$_{19}$-PANI-MWCNT Composite for Electromagnetic Interference (EMI) Shielding

Muhammad H. B. Zahari[1], Beh Hoe Guan[1, *], and Cheng Ee Meng[2]

Abstract—The salient individual properties of BaFe$_{12}$O$_{19}$, MWCNT, and PANI show promise in exhibiting excellent electromagnetic interference (EMI) shielding when they are combined. This research work focuses on developing a composite consisting of all three materials through a simple polymerization process and then evaluating its potential EMI shielding behaviour through electromagnetic measurements. The composite formation was morphologically and structurally verified through XRD, FTIR and FESEM measurements. The presence of main functional groups characteristic to PANI in the composite samples as shown by its FTIR spectra indicates its successful preparation through this method while FESEM micrographs show the random distribution of the composite constituents. The composite is conductive in nature with values reaching as high as 12.43 S/m for the composite with the highest MWCNT wt% (BPM_1_3_25). Electromagnetic measurements done at the X-band show promising EMI shielding behaviour in all prepared composites. The overall highest SE_A values are shown by sample BPM_1_3_25 with a minimum shielding value of 65 dB throughout the whole frequency band, far exceeding that of pure MWCNT.

1. INTRODUCTION

The search for economical and lightweight shielding materials continues with more focus put on studying various materials for both military and commercial applications [1–3]. Electromagnetic interference (EMI), a phenomenon in which disruptive electromagnetic energy is transmitted from one electronic device to another, used to be a major concern in military and radar technology. However, the rapid development of modern communication technology has exposed the commercial marketplace to the problem as more digital devices are made available to the general public. Since then, a lot of resources have been put into developing various methods of protection against EMI. A subset of the methods is the utilization of EMI shielding materials.

The current paradigm in developing shielding materials is to bring different materials with different salient electromagnetic properties together for the purpose of obtaining a single material that is able to exhibit optimum shielding properties, while taking advantage of the individual physical properties such as ease of fabrication and procurement, and also being cost effective. When evaluating the intrinsic parameters for the design of shielding materials, the following equation can be considered [4]:

$$A = 1/2\sigma E^2 + 1/2\omega\varepsilon_0\varepsilon_r E^2 + 1/2\omega\mu_0\mu_r H^2 \tag{1}$$

where A (W/m^3) is the electromagnetic energy absorbed per unit volume; E (V/m) is the electric field strength of the incident electromagnetic radiation; H (A/m) is the magnetic field strength of the incident electromagnetic radiation; σ (S/m) is the conductivity of the material; ω (sec^{-1}) is the angular speed of

* Corresponding author: Beh Hoe Guan (beh.hoeguan@utp.edu.my).
[1] Fundamental and Applied Sciences Department, Universiti Teknologi Petronas, Seri Iskandar, Perak Darul Ridzuan 32610, Malaysia.
[2] School of Mechatronic Engineering, Universiti Malaysia Perlis (UniMAP), Arau, Perlis 02600, Malaysia.

the electromagnetic wave ($\omega = 2\pi f$); ε_0 (F/m) is the dielectric permittivity of vacuum: 8.854×10^{-12} (F/m); ε_r is the complex permittivity of the material; μ_0 (A/m) is the magnetic permeability of vacuum: 1.2566×10^{-6} (A/m); and μ_r is the complex permeability of the material. As seen in Equation (1), the absorbing capability of a medium relies on parameters such as conductivity, complex permittivity, and complex permeability. These components are especially important as they would determine a materials' ability to dissipate energy through different magnetic and dielectric loss mechanisms. It is impossible to have a single shielding material that is able to encompass both magnetic and dielectric loss properties in one material. However, the combination of different materials is able to do so by combining it into composites.

Ferrites, especially the hexagonal type, have been considered as one of the most promising materials for microwave absorbing applications from the high demonstrated magnetic loss and wide absorption bandwidth. $BaFe_{12}O_{19}$, a member of the M-type hexagonal ferrite, is known for possessing high values of permeability in the microwave regions [5]. This is especially important as a higher value of complex permeability, especially its imaginary component, indicates a higher capability of the material to dissipate the absorbed electromagnetic energy in the form of heat through various magnetic loss mechanisms. Unfortunately, the practical application of $BaFe_{12}O_{19}$, as with other types of ferrites, is severely impeded by its heavy weight and low flexibility in molding it into complex structures [6]. This can be overcome by introducing an accompanying component that is lighter in weight and with considerable loss properties. Carbon-based materials lead this particular area with their light weight and higher surface area and have long been the subject of interest to be applied in many application as a result of their interesting properties. The conductive nature of multi-walled carbon nanotube (MWCNT) allows it to exhibit dielectric loss mechanisms. This, combined with the significantly larger value of its permittivity over other carbon allotropes makes MWCNT particularly appealing for EMI shielding applications. Despite this, the complex and costly fabrication process limits the widespread usage of MWCNT as a single shielding material [7]. A relatively cheaper supplementary component would be the family of conducting polymers. Polyaniline (PANI), a polymer belonging to this family, is particularly known for its economical and widely available precursor material, and relatively simple production methods. It functions similarly to that of MWCNT in which it is able to provide dielectric loss as a result of its high electrical conductivity σ. Despite both materials possessing significantly lighter weight than $BaFe_{12}O_{19}$, their application is limited due to poor magnetic loss and narrow absorbing bandwidth which again prevents the complete replacement of the magnetic component in a shielding material [8].

This research work details the integration of $BaFe_{12}O_{19}$, PANI, and MWCNT as a composite and its potential shielding properties. It is an attempt at optimising the combination of the three materials to further enhance its shielding capability and is an extension of our previous work [9]. The three components were brought together through a simple *in-situ* polymerization process. The structural and morphological aspects of the composite were characterized through XRD, FTIR and FESEM. The electrical properties of the composites were measured by using a 4-point resistivity measurement system. A network analyser and waveguide setup were employed to evaluate the EMI shielding properties of the prepared composites.

2. MATERIALS AND METHODS

2.1. Composite Preparation

$BaFe_{12}O_{19}$ powder was prepared through a typical sol-gel auto-combustion technique, as described elsewhere [10, 11]. MWCNTs (70–80% assay, *Sigma-Aldrich*) and the PANI monomer, aniline (99% purity, *R&M Chemicals*), were procured and used directly in the composite preparation process.

An example of the composite preparation is described as follows. Required amounts of $BaFe_{12}O_{19}$ and MWCNT were dispersed in 100 ml distilled water accompanied with vigorous stirring by an overhead stirrer. Separately, aniline, in the ratio of 1 : 10 to hydrochloric acid (HCl), was dispersed in HCl. Both mixtures were brought together in an ice bath and continuously stirred at 500 rpm. The polymerization process was initiated by adding pre-cooled ammonium persulfate solution (0.1 mol $(NH_4)_2S_2O_4$ in 100 ml distilled water). The ratio of aniline to $(NH_4)_2S_2O_4$ was set to 1 : 1.05. The mixture was allowed to react for 6 hours, with continuous stirring and the temperature maintained throughout the whole duration.

The reaction was terminated by filtering and repeatedly washing the as-obtained dark greenish-brown precipitate with ethanol and distilled water. The precipitate was oven-dried at 60°C for 48 hours. The composite preparation was then completed, and the samples are ready for the characterization process.

The samples tested in this work are divided into three main categories; single ($BaFe_{12}O_{19}$, PANI, and MWCNT), binary (BP_1_3) and ternary samples (BPM_1_3_5, BPM_1_3_15, and BPM_1_3_25). Table 1 lists the different composites prepared in this work. The designated sample name provides a rough idea on its composition. For example, for sample BPM_1_3_25, the 'BPM' notation implies that the sample is made up of $BaFe_{12}O_{19}$, PANI and MWCNT, while the '1_3_25' signifies the ratio between the components. In this sample, the ratio of $BaFe_{12}O_{19}$ to PANI is set to 1 : 3. The combination of the two ($BaFe_{12}O_{19}$+PANI) was then treated as a single entity, and its amount is then compared with MWCNT by taking the ratio of $BaFe_{12}O_{19}$+PANI to MWCNT as 75 : 25.

Table 1. Prepared samples with different component ratios.

Sample designation	Composite component ratio	
	$BaFe_{12}O_{19} : PANI$	$(BaFe_{12}O_{19}+ PANI) : MWCNT$
$BaFe_{12}O_{19}$	1 : 0	0 : 0
PANI	0 : 1	0 : 0
MWCNT	0 : 0	0 : 1
BP_1_3	1 : 3	1 : 0
BPM_1_3_5	1 : 3	95 : 5
BPM_1_3_15	1 : 3	85 : 15
BPM_1_3_25	1 : 3	75 : 25

2.2. Characterizations

Structural and morphological analysis were done through x-ray diffraction (XRD, Bruker A&S D8), Fourier-transform infrared spectroscopy (FTIR, Perkin Elmer), and Field-emission scanning electron microscope (FESEM, Supra 55VP ZeissVP-FESEM). A 4-point resistivity measurement system (Keithley 2400) was used to measure the electrical conductivity of the prepared composites. In order to perform electromagnetic testing on the composites, the powders were shaped into rectangular slabs with dimensions of 22.860 mm × 10.16 mm × 5 mm. The composite powders were mixed with 30% paraffin wax and were compacted in a rectangular mould by using a hydraulic press with an applied pressure of 5 kPa. The electromagnetic properties of the composites were evaluated by using a network analyser (Agilent Technologies E8362B PNA) at the X-band (8.2–12.4 GHz).

## 2.3. Shielding Effectiveness, SE

A wave, propagating from port 1 to port 2, when incident (1 = 100% power) on the surface of a medium with different impedances, would be split into three separate phases. Figure 1 details the wave propagation during the electromagnetic measurements.

A portion of the wave would be reflected (reflectance, R). Some would be absorbed within the medium of propagation (absorbance, A), and the remainder would transmit through (transmittance, T). Theses constants can be derived from the scattering parameters (S_{11}, S_{21}, S_{12}, S_{22}) through:

$$T = \left|\frac{E_T}{E_I}\right|^2 = |S_{12}|^2 (= |S_{21}|^2) \tag{2}$$

$$T = \left|\frac{E_R}{E_I}\right|^2 = |S_{11}|^2 (= |S_{22}|^2) \tag{3}$$

$$A = 1 = R - T \tag{4}$$
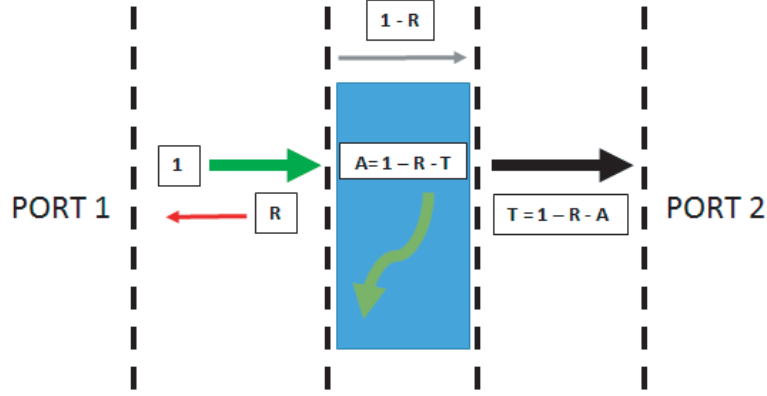
Figure 1. Wave propagation during network analyzer measurement.

The relative intensity of the electromagnetic wave propagating inside the medium after the reflection is given as $(1 - R)$. Therefore, the effective absorbance (A_{eff}), with respect to the intensity of the wave within the material can be expressed as:

$$A_{eff} = \frac{(1 - R - T)}{1 - R} \tag{5}$$

By expressing the terms in dB, the values of SE_A and SE_R can be obtained as:

$$SE_A = 10\log(1 - A_{eff}) = 10\log\left[\frac{T}{(1 - R)}\right] \tag{6}$$

$$SE_R = 10\log(1 - R) \tag{7}$$

As the effect of the multiple reflections, SE_M, is negligible when $SE_A \geq 10\,\mathrm{dB}$, the shielding performance depends only on the magnitude of shielding effectiveness through absorbance, SE_A and reflection, SE_R.

3. RESULTS & DISCUSSIONS

3.1. Structural and Morphological Characterization

Figure 2 illustrates the XRD patterns of $BaFe_{12}O_{19}$, PANI, MWCNT, BP_1_3 and BPM_1_3_15. As both PANI and MWCNT are non-crystalline materials, the diffraction pattern of the composite mirrors that of $BaFe_{12}O_{19}$. The $BaFe_{12}O_{19}$ peaks match perfectly with the standard diffraction pattern, ICSD 98-004-7018. Despite the prominent "hump" representing the semi-amorphous structure seen in the diffraction pattern of pure MWCNT, the same pattern was not observed in any of the composite samples. This can be attributed to its small amount within the composition and also to the overlapping with the amorphous hump of PANI at $2\theta = 20$–$30°$.

The successful polymerization of PANI in the composite preparation can be verified through FTIR measurement as shown in Figure 3. The FTIR spectrum for the composite mirrors closely that of pure PANI. The characteristic peaks of PANI can be observed at 1651, 1555, 1476, 1293, 1239, 1104, and $797\,\mathrm{cm^{-1}}$. The peak at $1651\,\mathrm{cm^{-1}}$ is attributed to the stretching vibrations of quinonoid, $-C = N$, and benzenoid, $-C = C$, at $1555\,\mathrm{cm^{-1}}$. The characteristic stretching vibrations of N-B-N (B = benzenoid ring) is depicted by the presence of the peak at $1476\,\mathrm{cm^{-1}}$. Peaks 1293 and $1239\,\mathrm{cm^{-1}}$ both correspond to the N-H bending vibration and the asymmetric C-N stretching vibration of the benzenoid rings while peak $1104\,\mathrm{cm^{-1}}$ refers to the N=Q=N (Q = quinonic type rings). The characteristic peak visible at $797\,\mathrm{cm^{-1}}$ is an effect of the out-of-plane C-H deformation vibration of the p-substituted benzene ring [12]. The presence of these characteristic peaks indicates the complete formation of PANI within the composite shielding material. Other characteristic peaks were also observed such as the characteristic peaks of the double bonds of the carbon nanotubes at $1632\,\mathrm{cm^{-1}}$ and $1384\,\mathrm{cm^{-1}}$ [13]. The intensity of
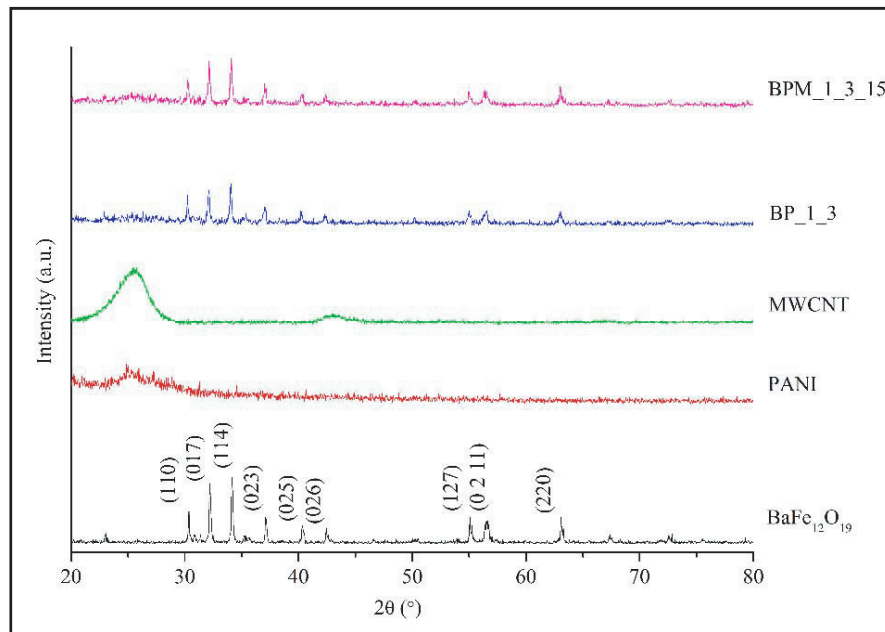
Figure 2. X-ray diffraction patterns of prepared composites.
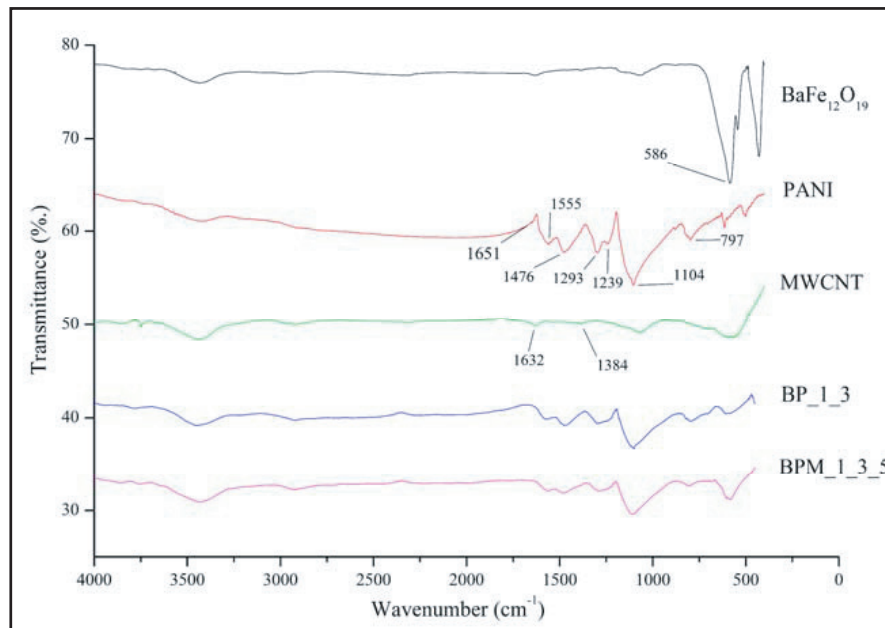

Figure 3. FTIR spectra of prepared composites.

the peaks of $BaFe_{12}O_{19}$ in the composites ($586\,\mathrm{cm}^{-1}$) is less intense than pure $BaFe_{12}O_{19}$ [14]. This is due to the effect of the coating of PANI on $BaFe_{12}O_{19}$ particle surfaces [15].

The resultant morphology from the $BaFe_{12}O_{19}$-PANI-MWCNT composite polymerization process is as shown in Figure 4. The three composite constituents possess distinct surface morphologies, making it easy to distinguish among each other as shown in the FESEM images of select samples in Figures 4(a)–(e). Figures 4(a), (b) and (c) consist of singular $BaFe_{12}O_{19}$, PANI and MWCNT while Figures 4(d) and (e) exhibit the composites BP_1_3 and BPM_1_3_15, respectively. Apart from the typical $BaFe_{12}O_{19}$ and
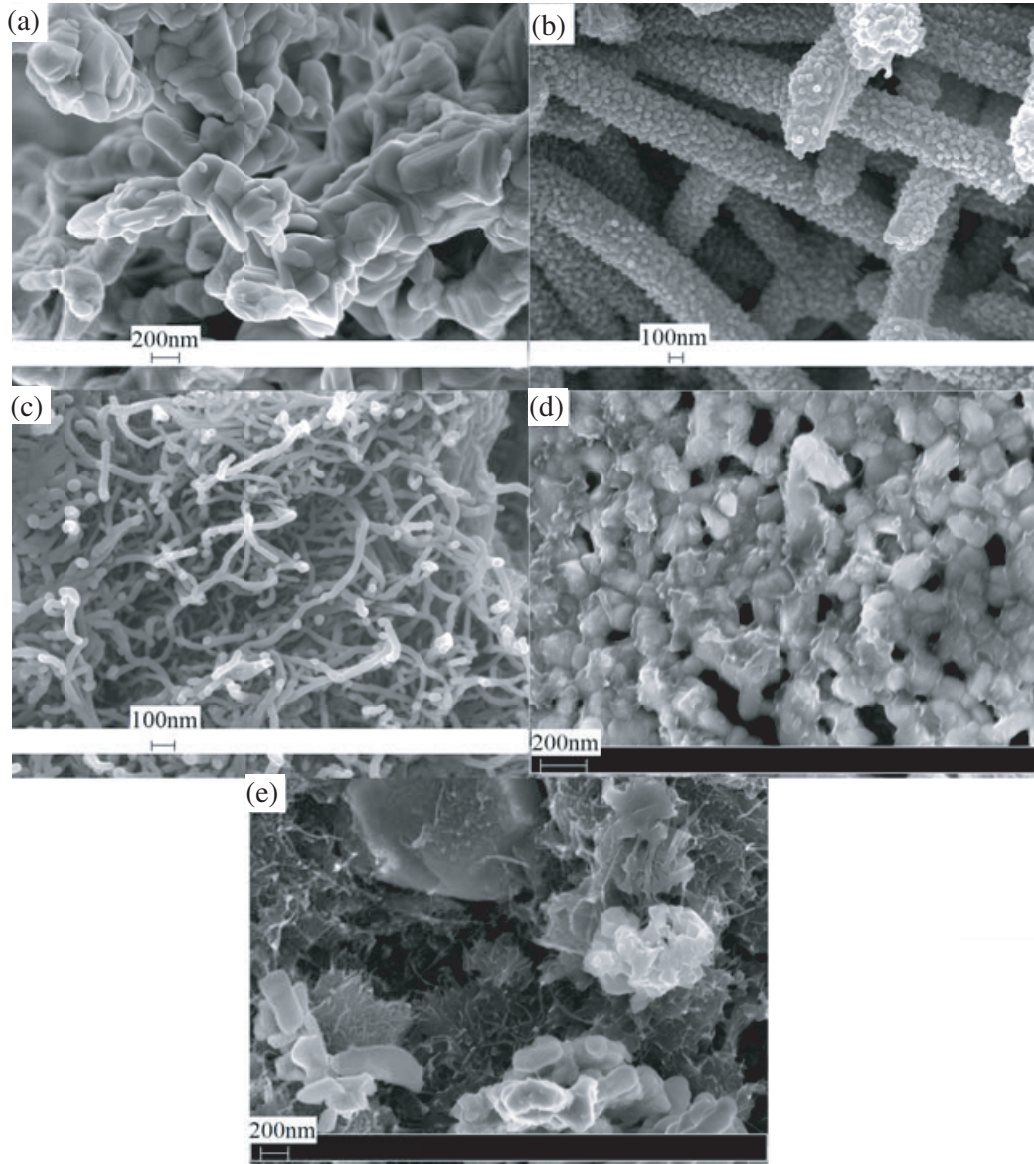
Figure 4. FESEM images of: (a) BaFe$_{12}$O$_{19}$, (b) PANI, (c) MWCNT, (d) BP_1_3, and (e) BPM_1_3_15.

MWCNT microstructures, it is interesting to note the stark difference in the particles of PANI, between when it was synthesized on its own and when it is polymerized together with the particles of BaFe$_{12}$O$_{19}$ and/or MWCNT. As observed in Figure 4(b), on its own, aniline has the tendency to polymerize into tubular structures [16]. The presence of foreign particles during the polymerization process would result in the aniline to polymerize on the particle surfaces, giving it a 'coating effect' which would facilitate the interconnectivity between particles. This is significantly important in creating a minimum loading level for MWCNT to form a continuous network of conducting particles, otherwise known as the electrical percolation threshold [17].

Figure 5 shows the result of the electrical conductivity measurement. As expected, the non-conductive BaFe$_{12}$O$_{19}$ possesses the lowest electrical conductivity with the value of 1.99×10^{-4} S/m. The electrical conductivity of MWCNT (not shown in Figure 5) far exceeds that of BaFe$_{12}$O$_{19}$ and PANI with a value of 197.77 S/m. The combination of BaFe$_{12}$O$_{19}$ and PANI puts the electrical conductivity of the BP_1_3 composite somewhere between the ferrite and conductive polymer. The addition of MWCNT into the mix leads to more than 5-fold increase in the electrical conductivity as seen in composite
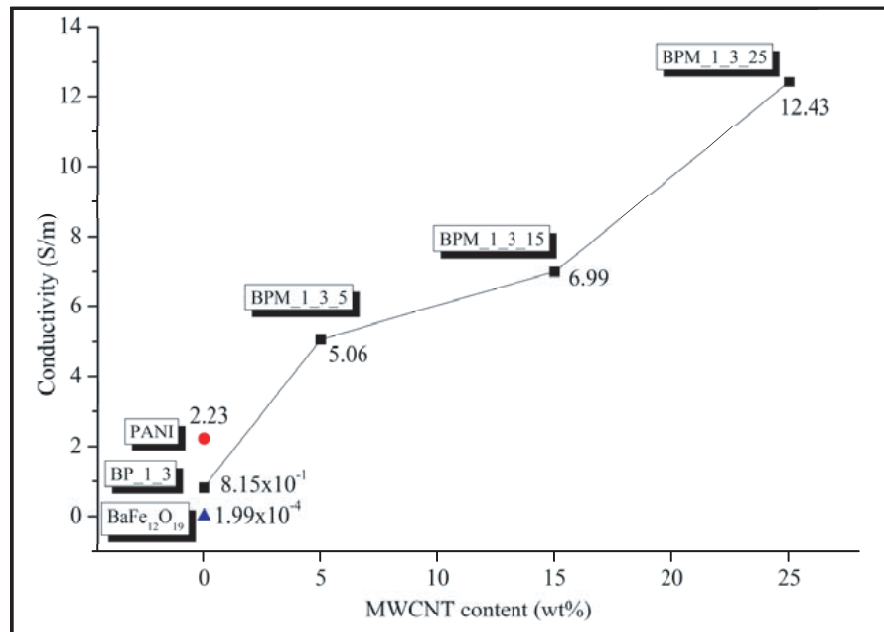
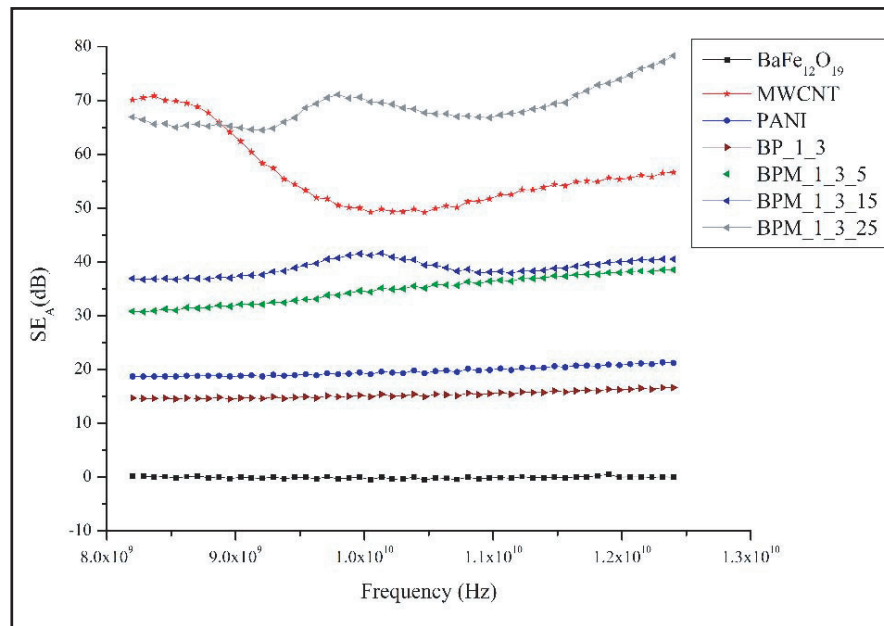**Figure 5.** Electrical conductivity of composite samples.

Figure 6. SE_A comparison between prepared samples.

BPM_1_3_5 and continues to increase further with each step increase of MWCNT wt%. This can be attributed to the interconnectivity between the particles especially to MWCNT and PANI. The high aspect ratio of the MWCNTs, coupled with the conductive PANI coating on both MWCNT and ferrite surfaces, facilitates the charge transfers between the conducting elements leading to the improvement of the electrical conductivity [18]. The highly conductive nature of the composites would give rise to dielectric losses, especially the conductance losses, which would play an important role in determining the electeromagnetic shielding properties of the composites.
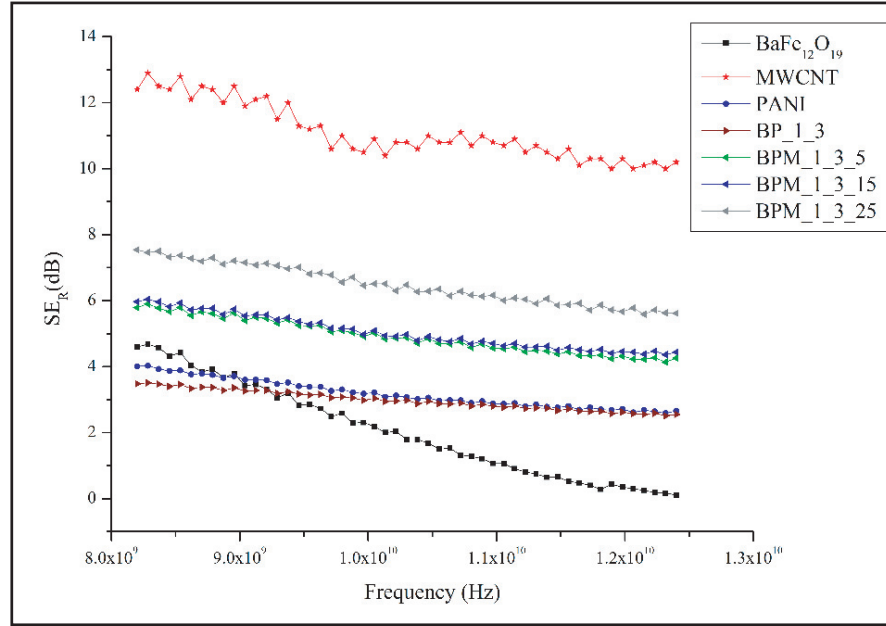
Figure 7. SE_R comparison between prepared samples.

The comparison between the shielding effectivenesses of measured samples in this research work is shown in Figures 6 and 7. When comparing among the 3 composite constituents ($BaFe_{12}O_{19}$, PANI, MWCNT), $BaFe_{12}O_{19}$ shows the poorest shielding performance with the SE_A values fluctuating above the 0 dB mark. A possible reason for this is the mismatch between the resonance frequencies for the optimum permeability values with the frequency range measured in this work. At microwave frequencies, the electromagnetic properties of magnetic materials is heavily reliant on its complex magnetic permeability, μ_r ($\mu_r = \mu' - j\mu''$). This constant determines the magnetic loss mechanism which in turn, affects the shielding properties greatly. In a study measuring the complex permeability of barium ferrite fibers, it was found that the natural resonance frequency for $BaFe_{12}O_{19}$ lies around 43.5 GHz [19]. However, it is possible to manipulate the material thickness and also pair it with different dielectric/conductive components to shift the resonance frequency to a lower frequency. The values of SE_A and SE_R exhibited by $BaFe_{12}O_{19}$ in this work imply that it is almost transparent to the incident electromagnetic energy. Thus, it can be inferred that the thickness and association with dielectric components used in this study are not an optimum combination for the ferrite to perform well at frequencies 8.2–12.4 GHz. This requires further study on the optimization of $BaFe_{12}O_{19}$ which is beyond the scope of this work. Pure MWCNT outperforms almost all of the measured samples in term of its SE_A and SE_R values. The highest SE_A for this material was observed at the frequency of 8.36 GHz with the value of 70.8 dB, while for the rest of the frequency band, more than 50 dB of SE_A was observed. This accounts for more than 99.99% of the wave energy propagating within the MWCNT solid sample being absorbed. This is not surprising considering the exceptionally high conductivity as compared to the other samples leading to enhanced dielectric losses. The SE_A values of PANI fall in between with values reaching 20 dB at frequencies between 10.8 and 12.4 GHz. The same phenomena were observed from the measured SE_R values of the materials. However, it is important to note that the SE_R for $BaFe_{12}O_{19}$ was slightly better than that of PANI between 8.24 and 8.78 GHz albeit dropping steadily as the frequency increases. This suggests that $BaFe_{12}O_{19}$, by itself, might be able to reflect electromagnetic waves better at lower frequencies.

The combination of $BaFe_{12}O_{19}$ and PANI results in its SE_A to fall slightly below PANI. Minimum values of 14 dB (SE_A) and 3 dB (SE_R) were observed throughout the X-band which translates to about 96.02% and 49.88% attenuations, respectively. The introduction of the MWCNT leads to a dramatic increase in the shielding effectiveness of $BaFe_{12}O_{19}$-PANI-MWCNT composites as compared to the $BaFe_{12}O_{19}$-PANI composite. At 5 wt% MWCNT, the SE_A and SE_R values of BPM_1_3_5 increased

to reach minimum values of 30 dB (99.90% attenuation) and 5 dB (68.38% attenuation), respectively. Further 10 wt% increase in MWCNT increases the shielding further. Finally, at 25 wt% MWCNT, the SE_A value of BPM_1_3_25 far exceeds all of the other samples, to the point that it is even able to outperform the shielding performance of MWCNT.

The composite samples have shown promising electromagnetic shielding properties where all composite samples were able to exhibit combined losses, both SE_A and SE_R, of more than 20 dB (99.00% attenuation). This was mainly attributed to the highly conductive nature of the composites. With respect to the classical electromagnetic theory, the shielding effectiveness due to absorption can be postulated through [20]:

$$SE_A = 20 \left(\frac{d}{\delta} \right) \log e = 20d \left(\frac{\omega \mu_r \sigma_{ac}}{2} \right)^{1/2} \log e \tag{8}$$

where d, δ, ω, μ_r, and σ_{ac} are the shield thickness, skin depth, angular frequency, complex magnetic permeability, and frequency dependent conductivity ($\sigma_{ac} = \omega \varepsilon_o \varepsilon''$), respectively. Equation (8) provides an insight to the intrinsic parameters that can be tailored to achieve optimum shielding performance through absorption. Aside from the electromagnetic parameters, μ and ε, electrical conductivity plays a prominent role in determining the shielding performance of a medium. The increased conductivity would give rise to conductance losses, among others. This is reflected in the form of the conductance loss tangent, $\mathrm{tg}\delta_c$ [8]:

$$\mathrm{tg}\delta_c = 1.8 \times 10^{10} \frac{\sigma}{f \varepsilon_r} \tag{9}$$

where σ, f, and ε_r are the electrical conductivity, frequency and complex permittivity, respectively. The combined effect from PANI and MWCNT leads to the enhancement of this dielectric loss mechanism. This was exemplified in sample BPM_1_3_25 surpassing the SE_A of MWCNT despite the higher value of electrical conductivity shown by MWCNT. Generally, a higher conductivity results in a higher shielding performance. However, it is also important to note that the impedance of materials with very high conductivity tends to be low. This will pose a problem if higher absorption performance is desired as the behavior of the conductive material approaches that of the metallic sheets where most of the wave will be reflected instead of being absorbed [8]. This suggests the existence of a threshold for the MWCNT wt% loading in composite materials for optimum shielding performance. The high values of SE_A and SE_R for composite BPM_1_3_25 show potential in utilizing the material in practical applications.

4. CONCLUSIONS

BaFe$_{12}$O$_{19}$-PANI-MWCNT composites were successfully developed. XRD, FTIR and FESEM confirm the successful formation of the composite through the *in-situ* polymerization process. The XRD pattern of the composite closely mirrors that of BaFe$_{12}$O$_{19}$. FTIR measurements revealed the presence of functional groups characteristic to each composite constituent. The micrographs taken using FESEM showed the random distribution of the particles within the composite matrix. The composites are highly conductive due to prominent amounts of PANI and MWCNT. This led to the enhanced shielding behavior shown by the composites. All composites measured in this research work were able to exhibit shielding values of more than 20 dB throughout the X-band with the highest SE_A value shown by sample BPM_1_3_25.

ACKNOWLEDGMENT

REFERENCES

1. Chung, D., "Electromagnetic interference shielding effectiveness of carbon materials," *Carbon*, Vol. 39, 279–285, 2001.

2. Jani, R. K., M. K. Patra, L. Saini, A. Shukla, C. P. Singh, and S. R. Vadera, "Tuning of microwave absorption properties and Electromagnetic Interference (EMI) shielding effectiveness of nanosize conducting black-silicone rubber composites over 8–18 GHz," *Progress In Electromagnetics Research M*, Vol. 58, 193–204, 2017.

3. Xing, D., L. Lu, W. Tang, Y. Xie, and Y. Tang, "An ultra-thin multilayer carbon fiber reinforced composite for absorption-dominated EMI shielding application," *Materials Letters*, Vol. 207, 165–168, 2017.

4. Tong, X. C., *Advanced Materials and Design for Electromagnetic Interference Shielding*, Taylor & Francis, 2008.

5. Li, L., K. Chen, H. Liu, G. Tong, H. Qian, and B. Hao, "Attractive microwave-absorbing properties of M-BaFe$_{12}$O$_{19}$ ferrite," *Journal of Alloys and Compounds*, Vol. 557, 11–17, 2013.

6. Pullar, R. C., "Hexagonal ferrites: A review of the synthesis, properties and applications of hexaferrite ceramics," *Progress in Materials Science*, Vol. 57, 1191–1334, 2012.

7. Wang, Y., T. Li, L. Zhao, Z. Hu, and Y. Gu, "Research progress on nanostructured radar absorbing materials," *Energy and Power Engineering*, Vol. 3, 580, 2011.

8. Huo, J., L. Wang, and H. Yu, "Polymeric nanocomposites for electromagnetic wave absorption," *Journal of Materials Science*, Vol. 44, 3917–3927, 2009.

9. Zahari, M. H., B. H. Guan, E. M. Cheng, M. F. Che Mansor, and K. C. Lee, "EMI shielding effectiveness of composites based on barium ferrite, PANI, and MWCNT," *Progress In Electromagnetics Research M*, Vol. 52, 79–87, 2016.

10. Xu, G., H. Ma, M. Zhong, J. Zhou, Y. Yue, and Z. He, "Influence of pH on characteristics of BaFe$_{12}$O$_{19}$ powder prepared by sol-gel auto-combustion," *Journal of Magnetism and Magnetic Materials*, Vol. 301, 383–388, 2006.

11. Liu, J., W. Zhang, C. Guo, and Y. Zeng, "Synthesis and magnetic properties of quasi-single domain M-type barium hexaferrite powders via sol-gel auto-combustion: Effects of pH and the ratio of citric acid to metal ions (CA/M)," *Journal of Alloys and Compounds*, Vol. 479, 863–869, 2009.

12. Quillard, S., G. Louarn, S. Lefrant, and A. MacDiarmid, "Vibrational analysis of polyaniline: A comparative study of leucoemeraldine, emeraldine, and pernigraniline bases," *Physical Review B*, Vol. 50, 12496, 1994.

13. Li, Y., Y. Huang, S. Qi, L. Niu, Y. Zhang, and Y. Wu, "Preparation, magnetic and electromagnetic properties of polyaniline/strontium ferrite/multiwalled carbon nanotubes composite," *Applied Surface Science*, Vol. 258, 3659–3666, 2012.

14. Xu, P., X. Han, and M. Wang, "Synthesis and magnetic properties of BaFe$_{12}$O$_{19}$ hexaferrite nanoparticles by a reverse microemulsion technique," *The Journal of Physical Chemistry C*, Vol. 111, 5866–5870, 2007.

15. Li, G., S. Yan, E. Zhou, and Y. Chen, "Preparation of magnetic and conductive NiZn ferrite-polyaniline nanocomposites with core-shell structure," *Colloids and Surfaces A: Physicochemical and Engineering Aspects*, Vol. 276, 40–44, 2006.

16. Zhang, L. and M. Wan, "Synthesis and characterization of self-assembled polyaniline nanotubes doped with D-10-camphorsulfonic acid," *Nanotechnology*, Vol. 13, 750, 2002.

17. Sandler, J., J. Kirk, I. Kinloch, M. Shaffer, and A. Windle, "Ultra-low electrical percolation threshold in carbon-nanotube-epoxy composites," *Polymer*, Vol. 44, 5893–5899, 2003.

18. Konyushenko, E. N., J. Stejskal, M. Trchová, J. Hradil, J. Kovářová, J. Prokeš, M. Cieslar, J.-Y. Hwang, K.-H. Chen, and I. Sapurina, "Multi-wall carbon nanotubes coated with polyaniline," *Polymer*, Vol. 47, 5715–5723, 2006.

19. Pullar, R., S. Appleton, and A. Bhattacharya, "The manufacture, characterisation and microwave properties of aligned M ferrite fibres," *Journal of Magnetism and Magnetic Materials*, Vol. 186, 326–332, 1998.

20. Verma, V., J. Kapil, and N. Singh, "Structural, magnetic properties of soft and hard ferrites and their EMI shielding application in X-band frequency range," *International Journal of Engineering Research & Technology (IJERT)*, 557–560, 2014.